

point, there is no net gain. For  $\eta < 0$ , which corresponds to electrons with a velocity  $v > V_0$ , the net result is a gain. This is the exact equivalent of the Stokes line in Raman scattering. For  $\eta > 0$ , the net result is absorption (anti-Stokes line).

The maximum gain is for  $\eta \simeq -\pi/2$ , and its value is

$$\alpha \simeq \frac{4 \times (256)}{\pi} r_0^2 \frac{n_e}{m c^2} \frac{k_i^{1/2}}{k_s^{3/2}} L^2 I_i. \quad (34)$$

This result has exactly the same functional form as that obtained by Sukhatme and Wolff,<sup>7</sup> who did a quantum electrodynamic calculation using the Dirac Hamiltonian, but is larger by a factor of 4. It is also within a factor of 0.8 of Madey's result.<sup>12</sup> This is very satisfying, if one considers the vastly different approximations performed in these different calculations.

In conclusion, we have shown that the free-electron laser is a completely classical device. The stimulated scattering producing amplification is due to electron bunching, rather than to the Compton recoil, as argued previously. This result not only is important from an academic viewpoint, but also greatly simplifies the analysis of the strong-signal regime and of the saturation of this new laser, as will be shown in a future publication.

We wish to thank Dr. J. M. J. Madey, Dr. W. E. Lamb, Jr., and Dr. F. Tappert for fruitful dis-

cussions.

\*Research supported by the U. S. Energy Research and Development Administration.

†Supported by Mathematics National Science Foundation Contract No. GT43070.

<sup>1</sup>P. L. Kapitza and P. A. M. Dirac, Proc. Cambridge Philos. Soc. 29, 297 (1933).

<sup>2</sup>L. R. Elias *et al.*, Phys. Rev. Lett. 36, 717 (1976).

<sup>3</sup>H. Dreicer, Phys. Fluids 7, 735 (1964).

<sup>4</sup>R. H. Pantell, G. Sonecini, and H. E. Puthoff, IEEE J. Quantum Electron. 4, 905 (1968).

<sup>5</sup>J. M. J. Madey, J. Appl. Phys. 42, 1906 (1971).

<sup>6</sup>J. M. J. Madey, H. A. Schwettmann, and W. M. Fairbank, IEEE Trans. Nucl. Sci. NS-20, 980 (1973).

<sup>7</sup>V. P. Sukhatme and P. W. Wolff, J. Appl. Phys. 44, 2331 (1973).

<sup>8</sup>W. Heitler, *The Quantum Theory of Radiation* (Oxford Univ. Press, Oxford, England, 1954).

<sup>9</sup>See for instance I. Lerche, in *Relativistic Plasma Physics*, edited by O. Buneman and W. B. Pardo (Benjamin, New York, 1968), p. 159.

<sup>10</sup>W. E. Lamb, Jr., Phys. Rev. 134, A1429 (1964).

<sup>11</sup>We note that this approximation must be used with care since it would indicate that the Stokes-anti-Stokes coupling is phase matched. However, an exact description of the field shows that this is not the case, i.e., the Stokes and anti-Stokes lines are not phase matched in stimulated scattering of electrons by a static periodic magnetic field.

<sup>12</sup>We note however, that the functional form of the gain is a direct consequence of Lorentz invariance. Consequently, all the physics is in the numerical factor. (J. M. J. Madey, private communication.)

## Rayleigh Scattering from Excited Atoms in Plasmas

W.-G. Wrobel, K.-H. Steuer, and H. Röhr

Max-Planck-Institut für Plasmaphysik, EURATOM Association, Garching, Federal Republic of Germany

(Received 16 August 1976)

Rayleigh and resonance scattering allow spatially resolved measurements of the neutral density and temperature in a plasma. While resonance scattering often is disturbed by line radiation of the plasma, this can be overcome by observation of near-resonant Rayleigh scattering. We performed scattering experiments at the 587.6-nm helium line using a flashlamp-pumped dye laser. The spectral dependence of the Rayleigh cross section and the polarization of the scattered light agree with theory.

In thermonuclear fusion experiments as well as in combustion diagnostics<sup>1</sup> or atmospheric research, one of the main diagnostic problems is the spatially resolved measurement of particle concentrations and temperatures. Resonant scattering at electronic transitions with tunable dye lasers offers high resolution and sensitivity since the cross section is very large. However, inelastic (quenching) collisions with rate  $\gamma_I$  decrease

the resonantly scattered intensity to a rather unknown level. Furthermore, in the case of high-particle concentration and low temperature, the scattering and surrounding medium may become optically thick in the line center and adsorb both laser and scattered radiation. In contrast to resonant scattering, these problems do not exist in near-resonant Rayleigh scattering.

The scattering cross section of bound electrons

with eigenfrequency  $\omega_0$  is given by <sup>2</sup>

$$\frac{d^2\sigma}{d\Omega_s d\omega_s} = \frac{\omega_L \omega_s^3 \langle 1 | \vec{e}_L \cdot \vec{d} | 2 \rangle \langle 2 | \vec{e}_s \cdot \vec{d} | 1 \rangle^2}{\hbar^2 c^4 [(\omega_L - \omega_0)^2 + \Gamma^2]} \left\{ \delta(\omega_L - \omega_s) + \frac{\gamma_E \Gamma}{\pi(\gamma_N + \gamma_I) [(\omega_s - \omega_0)^2 + \Gamma^2]} \right\}. \quad (1)$$

$\omega_L$  and  $\omega_s$  are the frequencies of incident and scattered light, respectively,  $\gamma_N$  is the radiative decay rate,  $\gamma_I$  and  $\gamma_E$  are the rates of inelastic and elastic collisions,  $\Gamma = \gamma_N + \gamma_E + \gamma_I$ , and  $\langle 1 | \vec{e}_L \cdot \vec{d} | 2 \rangle$  is a matrix element for the transition with eigenfrequency  $\omega_0$ . For  $|\omega_L - \omega_0| < \Gamma$ , Eq. (1) describes resonant scattering. In the case  $|\omega_L - \omega_0| > \Gamma$ , the spectrum of scattered radiation consists of two contributions. The first term describes Rayleigh scattering ( $\omega_L = \omega_s$ ), while the second one is due to collision-induced emission of light with frequency  $\omega_0$  and linewidth  $\Gamma$  (fluorescence).

By observation of only the Rayleigh-scattered light, there are at least four advantages in comparison to the observation of resonant scattering: (1) If the incident radiation is only slightly off-resonant, one benefits from the strong increase of the cross section, approaching the resonant value. (2) The cross section for Rayleigh scattering becomes independent of both the elastic ( $\gamma_E$ ) and the inelastic ( $\gamma_I$ ) collision rates if  $|\omega_L - \omega_0| > \Gamma$  [first term of Eq. (1)]. Collisions only determine the amount of the simultaneously emitted fluorescence at the line center [second term of Eq. (1)]; they have no effect on Rayleigh scattering.<sup>3</sup> (3) Resonant scattering becomes saturated when equal population of the involved levels is approached [not treated in (1)]. Saturation of Rayleigh scattering occurs at much higher levels of the incident light intensity.<sup>4</sup> Therefore, in most cases, the Rayleigh cross section is independent from the light intensity, which allows easy calibration of a scattering device by comparison with the Rayleigh scattering of a test gas. (4) The Rayleigh signal appears on a relatively low level of a continuum radiation while fluorescence is mixed with the strong line background radiation of the plasma or the reacting gas mixture.

The strong increase of the Rayleigh cross section approaching the emission wavelength can be

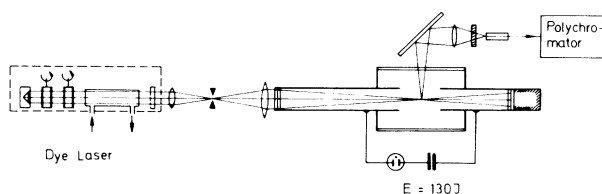


FIG. 1. Experimental setup for Rayleigh scattering with a tunable dye laser in a pulsed helium discharge.

observed best in media with narrow spectral lines, e.g., in glow discharges or low-pressure arcs. As a preparatory experiment for the detection of neutrals in thermonuclear fusion devices, we investigated Rayleigh scattering from excited atomic transition. The He I transition at 587.6 nm was chosen because of the emission maximum of our flashlamp-pumped rhodamine 6-G laser at 580 nm (pulse energy greater than 1 J, pulse width less than 5  $\mu$ sec, focus diameter 7.4 mm, linewidth 0.03 nm using two Fabry-Perot interferometers). The He atoms were excited in the positive column of a low-pressure arc (filling pressure 400 mTorr He) (Fig. 1). The scattered light emitted under 90° was analyzed by a fiber-optics multichannel polychromator in Littrow mounting with a resolution of 0.016 nm per channel and six photomultipliers. Figure 2 shows the spectrum of the He I line (full curve), the width of which is determined essentially by the resolution of the polychromator. The well-known splitting in the two components of 587.57 and 587.60 nm is just observable. The full circles show scattered light with the laser wavelength as the abscissa. Tuning the laser wavelength off resonance, the wavelength of scattered light changes in the same way. Its intensity decreases in agreement with theoretical predictions for the cross section [dashed curve  $\sigma \propto 1/(\Delta\lambda)^2$ ;  $\Delta\lambda$  is the laser detuning, with damping neglected]. There exists, however, a nonresonant region where the Ray-

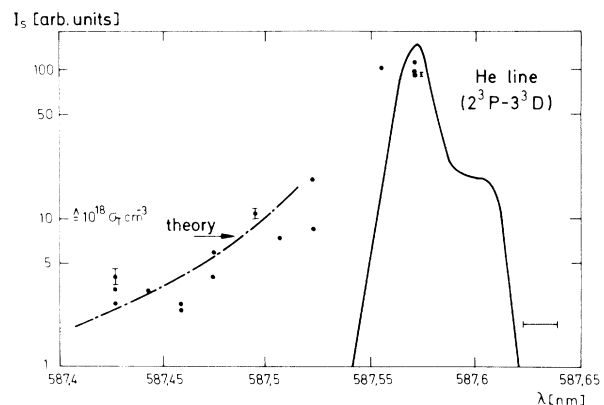


FIG. 2. Wavelength dependence of Rayleigh scattering signals (solid circles). Full curve, spectrum of spontaneous emission. Dashed curve, spectral dependence of Rayleigh scattering cross section.

leigh-scattered light is some orders of magnitude larger than the plasma radiation.

Along with earlier Rayleigh scattering experiments with excited atoms using fixed-frequency lasers,<sup>5</sup> we could prove the expected dependence of the cross section in the vicinity of the emission line. The density of the scattering atoms was determined by Rayleigh scattering of propane, the cross section of which was calculated from the pressure-dependent refractive index with the Clausius-Mosotti formula. With the formulas in Penney,<sup>6</sup> the cross section of the excited He atoms at 587.50 nm is  $\sigma = 3.81 \times 10^6 \sigma_T$ . The arbitrary value of intensity of  $I_s = 10$  in Fig. 2 corresponds to the scattering signal from 500 Torr propane, with a cross section equal to the

Thomson cross sections  $\sigma_T$  of  $10^{18} \text{ cm}^{-3}$  free electrons. Hence, the density of scattering He atoms should be  $2.6 \times 10^{11} \text{ cm}^{-3} \pm 20\%$ . The error is due to the shot noise of the photomultipliers. The reason for the variation of the scattering signals in Fig. 2 is the irreproducibility of the plasma. Estimates based on the data of our low-pressure arc yield densities in the same order of magnitude.

The prediction that light Rayleigh scattered under  $90^\circ$  should be completely polarized is only true if the scattering process starts from an initial state with angular-momentum quantum number  $J=0$ . This case has been investigated recently<sup>7</sup> at a Sr transition. For  $J \neq 0$ , however, the scattered light is only partially polarized<sup>8</sup> and the corresponding cross sections are,

$$\frac{d\sigma_{zz}}{d\Omega_s} = 9(2J+1)\omega_L^4 r_e^2 \sum_M \left\{ \sum_{T', J'} \frac{f_{TJ, T'J'}}{\omega_{TJ, T'J'}^2 - \omega_L^2} \begin{pmatrix} J' & 1 & J \\ -M & 0 & M \end{pmatrix} \right\}^2, \tag{2}$$

$$\frac{d\sigma_{xx}}{d\Omega_s} = \frac{9}{4}(2J+1)\omega_L^4 r_e^2 \sum_M \left\{ \sum_{T', J'} \frac{f_{TJ, T'J'}}{\omega_{TJ, T'J'}} \left[ \begin{pmatrix} J' & 1 & J \\ -M & 1 & M-1 \end{pmatrix} \begin{pmatrix} J' & 1 & J \\ -M & 0 & M \end{pmatrix} (\omega_{TJ, T'J'} - \omega_L)^{-1} \right. \right. \\ \left. \left. + \begin{pmatrix} J' & 1 & J \\ -M+1 & 0 & M-1 \end{pmatrix} \begin{pmatrix} J' & 1 & J \\ -M+1 & -1 & M \end{pmatrix} (\omega_{TJ, T'J'} + \omega_L)^{-1} \right] \right\}^2. \tag{3}$$

The scattering geometry (wave vectors  $\vec{k}_L$  and  $\vec{k}_s$ , and electric vectors  $\vec{e}_L$  and  $\vec{e}_s$  of the incident and scattered light, respectively) is described in Fig. 3. In Eqs. (2) and (3),  $T$  and  $T'$  specify the quantum numbers of the states involved except the angular momenta  $J$  and  $J'$ .  $f_{TJ, T'J'}$  is the oscillator strength of the transition and  $r_e = 2.818 \times 10^{-15}$  m. In our case (He I, 587.57 and 587.60 nm), we calculate with an oscillator strength of  $f = 0.609$  a degree of polarization

$$P = (\sigma_{zz} - \sigma_{xx}) / (\sigma_{zz} + \sigma_{xx}) = 0.65. \tag{4}$$

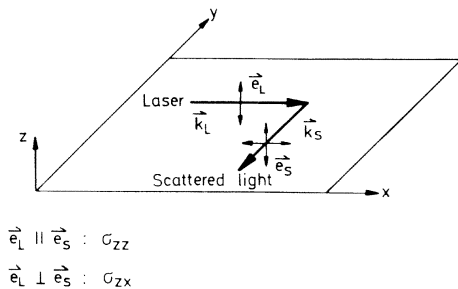


FIG. 3.  $90^\circ$ -scattering geometry and definition of scattering cross section for the two possible polarization directions.

Figure 4 shows our experimental results. Each datum point represents an average over ten shots. Resonance scattering is completely unpolarized, whereas the polarization of the Rayleigh-scattered light agrees with theory. To our knowledge, this is the first measurement of the degree of polarization of Rayleigh scattering by excited atoms.

To summarize, we have shown that in contrast

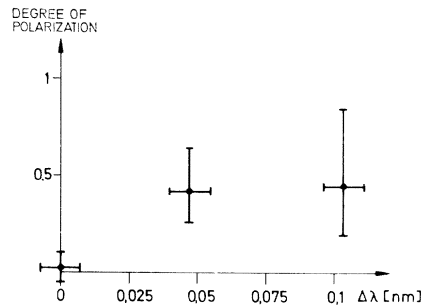


FIG. 4. Degree of polarization of resonant and Rayleigh-scattered light versus laser detuning from 587.6 nm.

to resonant scattering, Rayleigh scattering is insensitive to collisions, much to the advantage of possible diagnostic applications. We investigated Rayleigh scattering by excited atoms close to resonance. The wavelength dependence of the cross section and the degree of polarization agree with theory. A detailed report of our investigation will be given elsewhere.<sup>7</sup>

<sup>1</sup>D. Hartley, M. Lapp, and D. Hardesty, *Phys. Today* **28**, No. 12, 37 (1975).

<sup>2</sup>D. L. Rousseau, G. D. Patterson, and P. F. Williams, *Phys. Rev. Lett.* **34**, 1306 (1975).

<sup>3</sup>In the derivation of Eq. (1), the quasielastic collisions were treated in the impact approximation, which means that the duration of a single collision is short as compared to  $1/\omega_0$ . This approximation describes Stark

broadening by electrons (collisions of electrons and neutral atoms) and collisions between neutral atoms. As far as we know, the influence of ion broadening on Rayleigh scattering has not been treated theoretically. In the usual quasi-static model, the atomic energy levels are shifted and split by the Stark effect of the electric fields of the ions. The line shape is calculated from a statistical average over all perturbing ions. Their influence can be neglected if their contribution to line broadening is small compared to the spectral distance of laser and emission line, which is exactly the definition of Rayleigh scattering.

<sup>4</sup>B. R. Mollow, *Phys. Rev. A* **2**, 76 (1970).

<sup>5</sup>H. Röhr, *Z. Phys.* **225**, 494 (1969); H. F. Döbele and K. Hirsch, *Phys. Lett.* **54A**, 267 (1975).

<sup>6</sup>C. M. Penney, *J. Opt. Soc. Am.* **59**, 34 (1969).

<sup>7</sup>W.-G. Wrobel, Max-Planck-Institut für Plasmaphysik, D-8046 Garching, Internal Report IPP 1/160, 1976 (to be published).

<sup>8</sup>L. Vriens, *Phys. Lett.* **55A**, 331 (1976).

## Diamagnetism of a Simple Disordered System\*

J. M. Luttinger†

*The Rockefeller University, New York, New York 10021*

(Received 28 July 1976)

The diamagnetism of a model disordered system is calculated for low temperatures. If the magnetic field is not too large, the diamagnetic susceptibility per electron is large and proportional to  $T^{-2/5}$ . For large fields, however, this susceptibility rapidly decreases. A new variational method is used to obtain these results.

In a recent Letter<sup>1</sup> a new variational method for the partition function was described and applied to the calculation of the density of states of a model disordered system. In this note, the method is applied to the study of the diamagnetism of the same model. In particular, I shall limit myself to low temperatures and Maxwell-Boltzmann statistics (the sort of situation which might apply to some semiconductors under suitable conditions of doping and temperature) where the calculations are most transparent and where the effects are most interesting. We shall see that the diamagnetic susceptibility is large (per electron), and has a quite unusual field and temperature dependence.

As in the previous Letter<sup>1</sup> the electrons are assumed independent and described by a Hamiltonian ( $\hbar = m = 1$ )

$$\mathcal{H} = \frac{1}{2} [\vec{p} - (e/c)\vec{A}]^2 + v(\vec{r}), \quad (1)$$

where  $\vec{A}$  is the vector potential of the external

magnetic field and

$$v(\vec{r}) = u_{\text{wall}}(\vec{r}) + \sum_{j=1}^N u(\vec{r} - \vec{R}_j). \quad (2)$$

$u_{\text{wall}}$  is the potential which confines the particle to the volume  $V$  but is zero in  $V$ ,  $u(\vec{r})$  is a short-ranged potential without bound states, and the  $\vec{R}_j$  are the positions of the  $N$  scattering centers. The partition function  $Z$  is given by

$$Z = \text{Tr}[\exp(-\beta\mathcal{H})], \quad (3)$$

and its value averaged over the positions of the impurities is

$$\langle Z \rangle = \int_V \prod_j (d\vec{R}_j/V) Z. \quad (4)$$

Using the generalized coherent-state basis  $\psi(\vec{r}; \vec{P}, \vec{Q})$  for calculating the trace, proceeding exactly as in I [and taking the vector potential